Anal. Chem. **2008,** *80,* 1859−1864

Label-Free Detection of Melittin Binding to a Membrane Using Electrochemical-Localized Surface Plasmon Resonance

Ha Minh Hiep,[†,‡] Tatsuro Endo,[§] Masato Saito,[†] Miyuki Chikae,[‡] Do Kyun Kim,[†] Shohei Yamamura,[‡] Yuzuru Takamura,[‡] and Eiichi Tamiya*[,†,‡]

Department of Applied Physics, Graduate School of Engineering, Osaka University, Suita, Osaka 565-0871, Japan, School of Materials Science, Japan Advanced Institute of Science and Technology, 1-1, Asahidai, Nomi City, Ishikawa, 923-1292, Japan, and Department of Mechano-Micro Engineering, Interdisciplinary Graduate School of Science and Engineering, Tokyo Institute of Technology, 4259 Nagatsuta-cho, Midori-ku, Yokohama 226-8502, Japan

Localized surface plasmon resonance (LSPR) and electrochemistry measurements connecting to core−shell structure nanoparticle are successfully exploited in a simultaneous detectable scheme. In this work, the surface plasmon band characterizations of this nanostructure type are initially examined by controlling the core size of the silica nanoparticle and shell thickness of the deposited gold. These results clearly show that when the shell thickness is increased, keeping the core size constant, the peak wavelength of the LSPR spectra is shifted to a shorter wavelength and the maximum of peak intensity is achieved at a particular shell thickness. On the basis of this structure, we present a membrane-based nanosensor for optically detecting the binding of peptide toxin melittin to hybrid bilayer membrane (HBM) and electrochemically assessing its membrane-disturbing properties as a function of concentrations. It will open up the way to detect functionally similar protein toxins and other membrane-targeting peptides with the intension of integrating this chip into a microfluid and expanding it into multiarray format.

Deeper understandings of noble metal nanostructure phenomena are extremely important to develop the innovative nanosensors for biomolecular interactions. It is well-established that the metal nanostructures of particles, pore, rods, and rings have been investigated previously for plasmon properties as well as their highly sensitive and specific sensors for biological targets.[1,2] The term of localized surface plasmon resonance (LSPR) that results from the matching between the frequencies of incident photon and the collective oscillations of the conductive electron in the metal nanostructures has been potentially presented in the recent literature.[3−8] Theoretically, the absorbance sensing property of the LSPR is dependent upon the size, shape, and the spacing of nanostructures as well as their local environment.[9−14]

Pore-forming peptide toxins are cytolytic toxins that act on a plasma membrane for the purpose of permeabilizing the host cells.[15,16] Melittin, a noncell- selective lytic peptide from the venom of the honey bee has a direct effect on human erythrocytes lysis with the perturbation of the membrane,[17] leading to the hemoglobin leakage.[18] Importantly, melittin could exhibit its pore-forming effect on the mimic of natural membranes, providing a feasibly alternative way to detect and study some desirable properties in the artificial systems.[19,20]

A number of techniques to investigate the interactions of melittin toxin and the membrane have been detailed in the recent literature, including surface plasmon resonance (SPR),[21,22] electrochemical impedance spectroscopy,[23] second harmonic genera-

* To whom correspondence should be addressed. E-mail: tamiya@ap.eng.osaka-u.ac.jp. Phone: +81-6-6879-4087. Fax: +81-6-6879-7840.

[†] Osaka University.

[‡] Japan Advanced Institute of Science and Technology.

[§] Tokyo Institute of Technology.

(1) Link, S.; El-Sayed, M. A. *Annu. Rev. Phys. Chem.* **2003**, *54*, 331−366.
(2) Prasad, P. N. *Nanophotonics*; Wiley-Interscience: New York, 2004.
(3) Kelly, K. L.; Coronado, E.; Zhao, L.; Schatz, G. C. *J. Phys. Chem. B* **2003**, *107*, 668−677.
(4) Hutter, E.; Fendler, J. H. *Adv. Mater.* **2004**, *16*, 1685−1706.
(5) Prodan, E.; Nordlander, P.; Halas, N. J. *Nano Lett.* **2003**, *3*, 1411−1415.
(6) Stuart, D. A.; Haes, A. J.; Yonzon, C. R.; Hicks, E. M.; Van Duyne, R. P. *IEEE Proc. Nanobiotechnol.* **2005**, *152*, 13−32.
(7) Freeman, R. G.; Grabar, K. C.; Allison, K. J.; Bright, R. M.; Davis, J. A.; Guthrie, A. P.; Hommer, M. B.; Jackson, M. A.; Smith, P. C.; Walter, D. G.; Natan, M. J. *Science* **1995**, *267*, 1629−1632.
(8) Nath, N.; Chilkoti, A. *Anal. Chem.* **2004**, *76*, 5370−5378.
(9) Sherry, L. J.; Jin, R.; Mirkin, C. A.; Schatz, G. C.; Van Duyne, R. P. *Nano Lett.* **2006**, *6*, 2060−2065.
(10) Sherry, L. J.; Chang, S. H.; Schatz, G. C.; Van Duyne, R. P.; Wiley, B. J.; Xia, Y. *Nano Lett.* **2005**, *5*, 2034−2038.
(11) Huang, W. Y.; Qian, W.; El-Sayed, M. A. *Nano Lett.* **2004**, *4*, 1741−1747.
(12) Nath, N.; Chilkoti, A. *Anal. Chem.* **2002**, *74*, 504−509.
(13) Mock, J. J.; Smith, D. R.; Schultz, S. *Nano Lett.* **2003**, *3*, 485−491.
(14) Himmelhaus, M.; Takei, H. *Sens. Actuators, B* **2000**, *63*, 24−30.
(15) Parker, M. W.; Feil, S. C. *Prog. Biophys. Mol. Biol.* **2005**, *88*, 91−142.
(16) Lehrer, R. I.; Ganz, T. *Curr. Opin. Immunol.* **1999**, *11*, 23−27.
(17) Tosteson, M. T.; Holmes, S. J.; Razin, M.; Tosteson, D. C. J. *Membr. Biol.* **1985**, *87*, 35−44.
(18) Naito, A.; Nagao, T.; Norisada, K.; Mizuno, T.; Tuzi, S.; Saito, H. *Biophys. J.* **2000**, *78*, 2405−2417.
(19) Habermann, E. *Science* **1972**, *177*, 314−322.
(20) Andersson, A.; Biverstah, H.; Nordin, J.; Danielsson, J.; Lindah, E.; Maler, L. *Biochim. Biophys. Acta* **2007**, *1768*, 115−121.
(21) Papo, N.; Shai, Y. *Biochemistry* **2003**, *42*, 458−466.
(22) Mozsolits, H.; Wirth, H. J.; Werkmeister, J.; Aguilar, M. I. *Biochim. Biophys. Acta* **2001**, *1512*, 64−76.
(23) Becucci, L.; Leon, R. R.; Moncelli, M. R.; Rovero, P.; Guidelli, R. *Langmuir* **2006**, *22*, 6644−6650.

10.1021/ac800087u CCC: $40.75
Published on Web 02/23/2008

tion,[24] and cantilever array sensor.[25] The combination of SPR and electrochemistry in a planar gold surface, electrochemical surface plasmon resonance (ESPR), archived a highly sensitive, reliably complementary analysis of the toxin−membrane interactions at fully identical experimental conditions.[26,27] However, the requirement of the Kretschmann configuration in its total internal reflection mode limits the possibilities for massively parallel detection in a miniaturized package as well as lab-on-a-chip incorporation. The surface plasmon band excitation of the core−shell nanostructure substrates in a simple collinear optical system has been previously demonstrated as the potential model to overcome these limitations.[28−32] Different from the fabrication of gold nanoparticles in solution, this nanostructure was suitable to process in various flexible formats, an important property to develop completed biochips in analytical and biosensor applications. In its construction, the silica nanoparticles were used as the "core" and thin gold films were used as the "shell" coated at the bottom and the top of the "core". Therefore, the excitation mode of the plasmon absorption spectra of the core−shell nanoparticle structure could be auspiciously controlled by changing the size of the silica nanoparticle and the shell thickness of the gold layer. Additionally, the LSPR microfluidic format was also developed, thus giving an excellent possibility to integrate LSPR measurement into micrototal analysis systems (μTAS).[33] These previous achievements encouraged us to apply our core−shell structure nanoparticle structure to develop an electrochemical-localized surface plasmon resonance (E-LSPR) sensor for the possible detection of peptide toxin.

In this work, we obviously examine the optical absorption properties of the core−shell nanoparticle structure throughout the visible region with controlling the core size of the silica nanoparticles and the shell thickness of the deposited gold layer using UV−vis spectroscopy. The peak intensity and wavelength of the LSPR spectra behaviors were closely related to the size of the silica nanoparticle and the thickness of the deposited gold layer. Subsequently, the core size of 100 nm and the shell thickness of 29 nm were used to optically and electrochemically estimate the biomolecular interactions between melittin and the hybrid bilayer membrane (HBM). The binding of melittin to HBM was measured using localized surface plasmon resonance, and the permeability of the HBM was then assessed electrochemically as a function of melittin with the purpose of seeking a novel, sensitive detection system for peptide toxins.

(24) Kriech, M. A.; Conboy, J. C. *J. Am. Chem. Soc.* **2003**, *125*, 1148−1149.
(25) Pera, I.; Fritz, J. *Langmuir* **2007**, *23*, 1543−1547.
(26) He, L.; Robertson, J. W. F.; Li, J.; Karcher, I.; Schiller, S. M.; Knoll, W.; Naumann, R. *Langmuir* **2005**, *21*, 11666−11672.
(27) Bart, M.; Van Os, P. J. H. J.; Kamp, B.; Bult, A.; Van Bennekom, W. P. *Sens. Actuators, B: Chem.* **2002**, *84*, 129−135.
(28) Endo, T.; Kerman, K.; Nagatani, N.; Ha, M. H.; Kim, D. K.; Yonezawa, Y.; Nakano, K.; Tamiya, E. *Anal. Chem.* **2006**, *78*, 6465−6475.
(29) Endo, T.; Kerman, K.; Nagatani, N.; Takamura, Y.; Tamiya, E. *Anal. Chem.* **2005**, *77*, 6976−6986.
(30) Kim, D.-K.; Kerman, K.; Saito, M.; Sathuluri, R. R.; Endo, T.; Yamamura, S.; Kwon, Y.-S.; Tamiya, E. *Anal. Chem.* **2007**, *79*, 1855−1864.
(31) Ha, M. H.; Endo, T.; Kerman, K.; Chikae, M.; Kim, D. K.; Yamamura, S.; Takamura, Y.; Tamiya, E. *Sci. Technol. Adv. Mater.* **2007**, *8*, 331−338.
(32) Vestergaarda, M.; Kerman, K.; Kim, D. K.; Ha, M. H.; Tamiya, E. *Talanta* **2008**, *74*, 1038−1042.
(33) Ha, M. H.; Endo, T.; Kim, D. K.; Tamiya, E. *Proc. SPIE* **2007**, *6768*, 67680I1−67680I11.

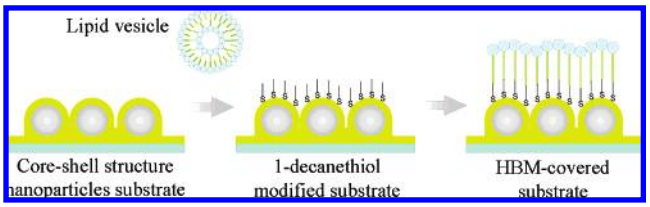

Figure 1. Fabrication of the membrane-based sensor using the core−shell structure nanoparticle substrate.

EXPERIMENTAL SECTION

Materials. Gold (1 mm in diameter) was purchased from Kuruya Metal Co., Ltd (Tokyo). Silica nanoparticles in various diameters of 50, 100, 150 nm were obtained from Polysciences Inc. (Warrington, PA). 3-Aminopropyltriethoxysilane (γ-APTES) from Shin-Etsu Chemical Co., Ltd. (Tokyo, Japan) was used for surface modification of the silica nanoparticles. 4,4′-Dithiodibutyric acid (DDA) for self-assembled monolayer (SAM) formation on the gold substrate surface was purchased from Aldrich. 1-Ethyl-3-(3-dimethylaminopropyl)carbodiimide (EDC) for the activation of the carboxyl group of DDA was supplied by Dojindo Laboratories (Kumamoto, Japan). Electronic grade sulfonic acid and hydrogen peroxide for cleaning the slide substrates were purchased from Kanto Kagaku (Tokyo, Japan). All other reagents were analytical reagent grade, and solutions were prepared with ultrapure water (18.3 MΩ cm) obtained from Millipore.

Fabrication of Core−Shell Structure Nanoparticle Substrate. The approach for fabricating the core−shell structure nanoparticles substrate was developed previously.[31] Briefly, the silicon slides were used to deposit of a chromium layer of 5 nm and a gold layer of 30 nm in succession with the use of a plastic mask contained two parts, a ring part (diameter, 3 cm) and a line part. Silica nanoparticles (50, 100, 150 nm in diameter) which were modified with amino groups on their surface by reaction with 1% (v/v) γ-APTES solution could then form esters with carboxyl groups of 4, 4′-dithiodibutyric acid in the ring part of the gold substrate, producing the nanoparticles monolayer. Later deposition of a thin gold-cap layer and separation of the nanoparticle area with an insulated tape could complete the fabrication process of the substrate. This core−shell structure nanoparticle substrate could be used simultaneously as a working gold electrode and LSPR-exciting device. All electrochemical measurements were performed by using a three-electrode system with a platinum wire as the counter electrode and an Ag/AgCl electrode as the reference electrode.

HBM Formation and the Melittin−Membrane Interaction Measurements. The lipid vesicles were prepared from dissolving dimyristoylphosphatidylcholine (DMPC, Sigma) in pure chloroform. The organic solvent was then removed with a N_2 stream to form a thin lipid layer, and the samples were kept continuously in a vacuum desiccator for 12 h. An amount of a 0.01 M phosphate buffer saline (pH 7.5, containing 0.1 M NaCl) was added, giving a final lipid concentration of 0.5 mg/mL. The lipid vesicle solution was then sonicated for 1 h and used within 24 h.

A self-assembled alkanethiol layer was archived by introducing 1 mM decanethiol (Wako) solution onto the substrate surface for 1 h. After fusing the lipid vesicles on the alkanethiol-modified surface for 2 h (Figure 1), the hybrid bilayer membrane-immobilized surface was exposed to negative control BSA (100

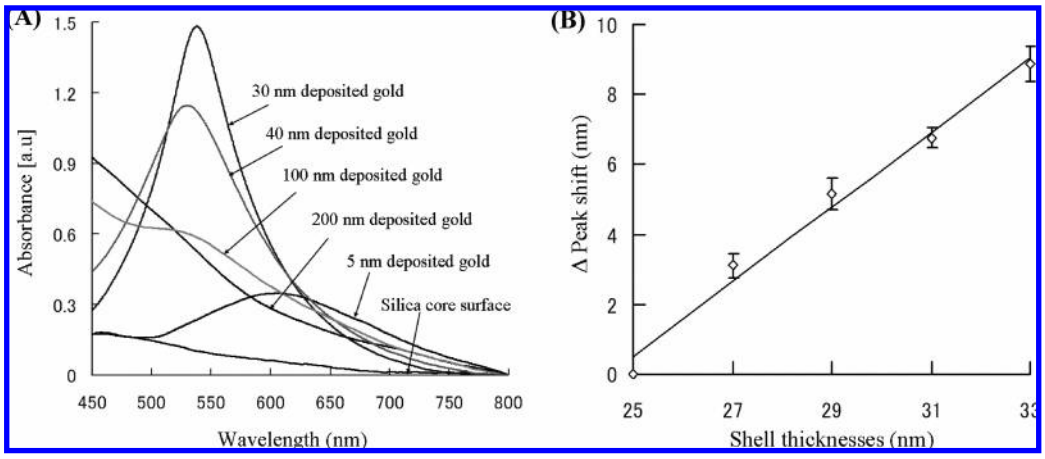

Figure 2. (A) Shell thickness dependence of plasmon absorption on the silica nanoparticle layer substrate surface and (B) plot of Δpeak shift versus shell thicknesses in a range from 25 to 33 nm.

μg/mL in PBS buffer) to confirm the complete coverage of the nonspecific binding sites. Then aliquots of 20 μL of the melittin solutions were introduced for 20 min, and the E-LSPR measurements were continuously performed.

RESULTS AND DISCUSSIONS

Nanoparticle Structure Formation and Shell Thickness Dependence of Plasmon Absorption. The wavelength and intensity tunability of the LSPR spectrum in the visible region (400−800 nm) were investigated in this study. These have been performed by varying the size of the silica nanoparticle (core size) and the deposited-gold layer (shell thickness) of the nanoparticle structure. Figure 2A illustrated the absorbance spectra with different shell thicknesses on the silica nanoparticle substrate. On the basis of the silica nanoparticle of 100 nm in diameter, the significant increases in the LSPR spectrum was observed when various gold thicknesses were deposited on the surface. Moreover, the red shift of the peak wavelength was clearly recorded. In order to attain a better evaluation of the LSPR peak shift, a larger shell thickness range from 25 to 33 nm was analyzed. As a result, a high linear range from 542 to 551 nm was reached, as shown in the Figure 2B. The shell thickness sensitivity corresponding to peak wavelength yielded a constant of 0.11; the increasing of 10 nm in the gold layer produces a decrease of 1.1 nm of the LSPR peak wavelength. Our results were in agreement with the red shift behaviors in the LSPR peak wavelength versus nanoparticle heights in the previous reports.[2]

The peak absorbance intensity of the LSPR spectra was also analyzed in detail. No peak of the LSPR spectra appeared in the bare silica core substrate. Deposition of 5 nm in gold thickness on the surface caused the increase in the peak absorbance spectrum due to the slight initial capping of gold on the nanoparticle core substrate. Comparing to a relatively lager size of the core, an extremely thin film seemed to not be enough to cover all of the silica nanoparticles to make a uniform core−shell nanoparticle structure surface. The growing of the gold layer deposited by the evaporation technique caused a considerable enhancement in the peak intensity of the LSPR spectrum. These results suggested two things: (1) a strong enhancement of the local electromagnetic field surrounding the core−shell nanoparticle due to the interaction of the electromagnetic radiation of incident light with the free electrons in the metal−shell part and (2) the enhanced couplings between the relatively closed core−shell nanoparticles due to the random monolayer formation of surface-modified silica nanoparticle on the thiol-functionalized surface. However, the deeper deposition of the 100 nm gold thickness caused the vigorous contact in the shell of the closed nanoparticle and changed the shape of the surface of the core−shell nanoparticle structure, resulting in the drastic reduction in the peak intensity and broadening the bandwidths of the LSPR spectra (the AFM images were shown in the Supporting Information). The peak intensity of the LSPR spectrum almost dispersed because the shell thickness of 200 nm was prepared.

Core Size Dependence of Plasmon Absorption. The peak intensities of the LSPR spectra response were also estimated in three core sizes (50, 100, and 150 nm) with the larger range of shell thicknesses (Figure 3A). For the smaller core, the thinner shell thickness is required to excite the maximum peak intensity which is probably to be corresponded with a best uniform formation of core−shell nanoparticle structure. As the result, the optimal peak intensities of the LSPR spectra were recorded from 23 nm (core size of 50 nm), 29 nm (core size of 100 nm), and 31 nm (core size of 150 nm) in shell thicknesses. In all these cases, both the lower and higher shell thickness caused the decreases in the peak intensity of the surface plasmon band. As in the discussions above, these could be interpreted as either not enough shell thickness for covering all the core nanoparticles or the inhibitions of the local electromagnetic field of the nanoparticles caused by a highly dense gold layer. The obvious red shifts of the maximum peak intensity from 477.5 to 539.46 to 569.04 nm was obtained when the core size increases, correspondingly, from 50 to 100 to 150 nm. Consequently, the core size sensitivity was calculated with a constant of 0.91, an increase of 10 nm in the core diameter produces an increase of 9.1 nm in the LSPR peak wavelength (Figure 3B). The reasons for the red shift of the LSPR spectra in the larger core−shell nanoparticles could be theoretically considered that the polarization of incident light to nanoparticles is in the high-order mode but not in homogeneous one. These higher-order modes peak at lower energy, and thus the red shift of the plasmon band increases with increasing nanoparticle size. The plasmon absorbance data of the core−shell

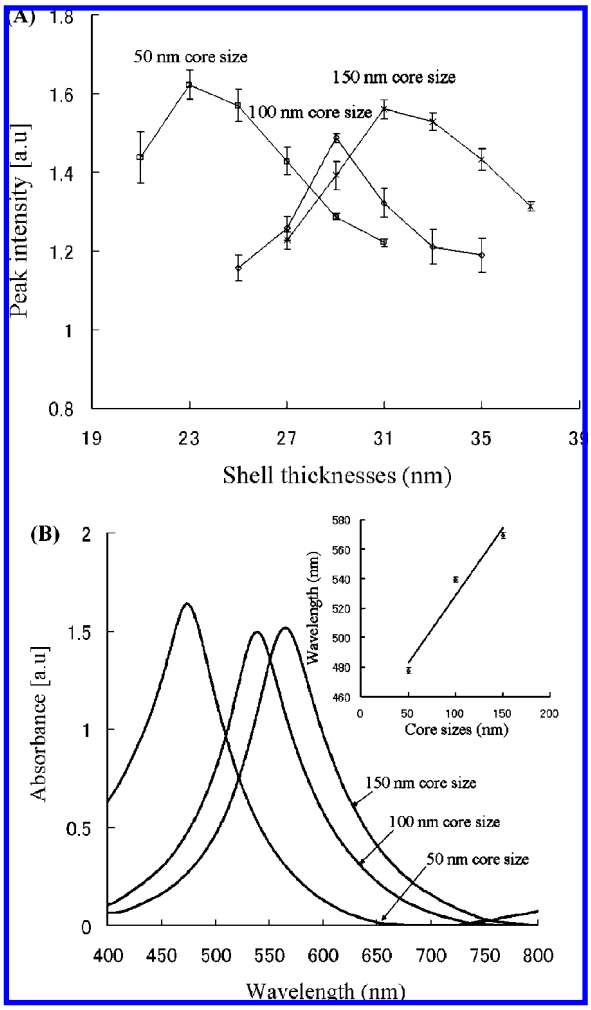

Figure 3. (A) The peak intensity and (B) peak wavelength characterizations of the LSPR spectra for three core sizes of 50, 100, and 150 nm in diameter.

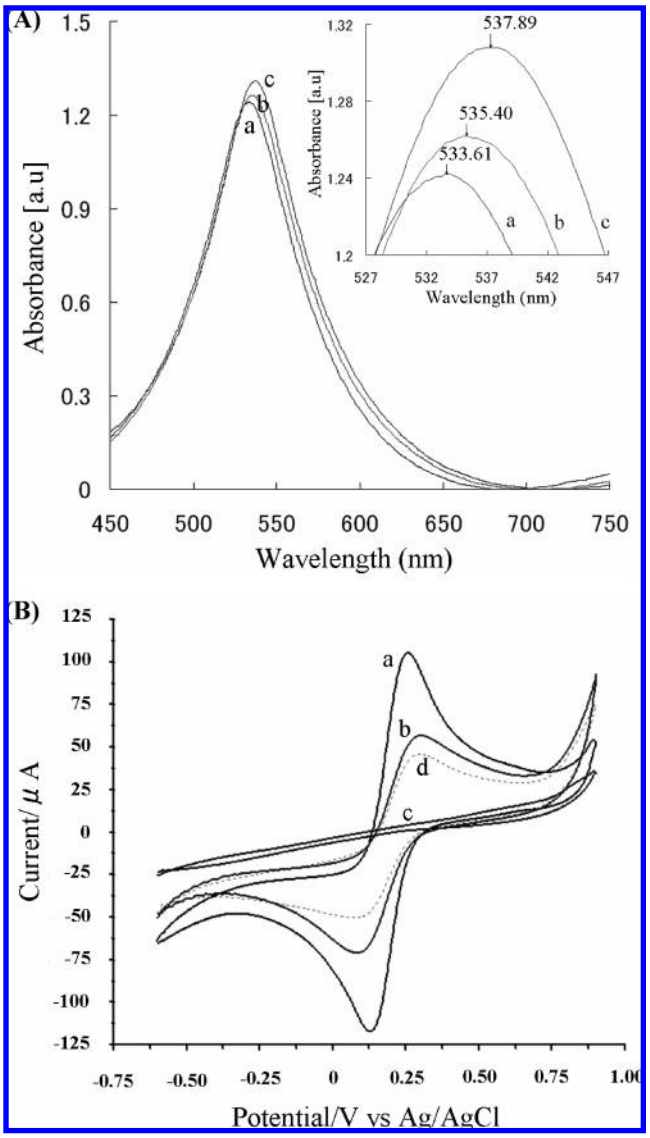

Figure 4. (A) The peak absorbance intensity increases and the peak-shift of the core−shell structure nanoparticle substrate due to the successive depositions steps: (a) bare substrate, (b) 1-decanethiol-modified surface, and (c) HBM-covered surface. (B) Cyclic voltammogram of the core−shell structure nanoparticle substrate (a), of the thiol-modified substrate (b), of the HBM-covered substrate (c), and after incubation with 100 ng/mL melittin (d) in 2 mM $[Fe(CN)_6]^{3-/4-}$. The electrode solution contained 20 mM phosphate buffer (pH 7.4) and 100 mM KCl. The scan rate was 100 mV/s.

nanoparticle structure is clearly visible and follows the predicted behavior for the cases of gold nanoparticles and another type of core−shell nanostructures.[2]

LSPR and Electrochemical Behaviors of HBM. The optical and electrochemical characteristics of the core−shell structure nanoparticles substrates were evaluated using a simple collinear optical system and Autolab PGSTAT 100 system. The absorbance peak at ~530 nm and the typical cyclic voltammogram of this substrate were clearly observed due to the rather regular nanoparticles surface, thus allowing performance of LSPR and electrochemistry analyses on the same surface.

The LSPR behaviors of the core−shell structure nanoparticle substrate were investigated corresponding to the HBM deposition steps (Figure 4A). Compared to the bare substrates, the absorbance spectra of the alkanethiol-modified ones were changed with an average peak shift of 2.03 nm and an absorbance strength increase of 0.02 absorbance units (AU) due to the self-assembly formation of 1-decanethiol on the gold surface. Both the peak shift and the increase in absorbance of the core−shell structure nanoparticle substrates could be used as the optical signatures for studying biomolecular interactions. Because of slightly higher sensitivity, we focused on monitoring the absorbance intensity changes in the LSPR response in this study. Dispersed with a lipid vesicle solution, the alkanethiol-modified hydrophobic surface could be contacted with acyl chains of polar lipids, orienting its polar headgroups toward the solution. As the result, the formation of HBM caused an intensive increase in the LSPR spectrum by about 0.039 (AU) in comparison to the decanethiol-modified surface. The similar optical changes of the surface plasmon properties were previously reviewed when other types of lipid vesicles were formed as a monolayer on the flat gold surface.[34,35]

On the other hand, the presence of 1-decanethiol and successive DMPC layers on the bare substrate surface strongly sup-

(34) Li, A.; Ma, Y.; Fan, Y.; Xiurong, Y. *Appl. Surf. Sci.* **2007**, *253*, 6103−6108.

(35) Besenicar, M.; Macek, P.; Lakey, J. H.; Anderluh, G. *Chem. Phys. Lipids* **2006**, *141*, 169−178.

pressed the electrochemical reaction of the redox probes. As shown in Figure 4B, a decrease in the magnitude and an insignificant change in the peak separation archived from the 1-decanethiol modified substrate surface presumed that the 1-decanethiol layer was not densely packed, thus maintaining the permeability for the electroactive species. Formation of HBM on the surface noticeably prevented the access of the redox probe and considerably restrained the faradaic current, resulting in a relatively flat-shaped curve. This result evidently demonstrated that the formation of the DMPC layer on the core−shell structure nanoparticle surface mostly blocked the interfacial electron transfer between the redox probe and the gold surface. Consequently, HBM had been successfully prepared on the gold surface, creating a simple membrane-based sensor from the core−shell structure nanoparticle substrate.

Measurements of Membrane-Based Sensor for Peptide Toxin. The absorbance strength increments in the LSPR response of the sensor were observed when various melittin concentrations of 0, 5, 10, 50, 100, and 500 ng/mL were independently introduced onto the membrane-based sensors. Each concentration was repeated four times. The slight absorbance peak increments in the buffer solution (without melittin) was a result of physical binding but not by melittin peptide. With the higher concentrations of melittin, the peak absorbance intensities of the LSPR spectra were increased constantly, denoting the interactions of melittin with HBM, and the amount of bound melittin was directly related to the peptide toxin concentrations (Figure 5A). The LSPR measurement appears to be highly sensitive for detection of low toxin concentrations. Even at 10 ng/mL melittin, a distinct response in the peak absorbance intensity increase could be obtained. Our results were in agreement with the previous study in which a few nanograms per milliliter of melittin could bind to an artificial membrane using the surface plasmon resonance method.[21]

Moreover, when a melittin solution of 100 ng/mL was introduced onto the HBM modified surface, the amperometric response of $[Fe(CN)_6]^{3-/4-}$ was considerably increased (Figure 4B). This enhancement suggested that the melittin could interact with the mimic biomembrane, causing the leakage of this layer. The relation between the HBM disturbance and the amount of melittin peptide was established when a series of melittin concentrations (50, 100, and 500 ng/mL) were applied. The higher were toxin peptide concentrations, the stronger were the disturbances that occurred, thus evidently expressed by the enhancement of their cyclic voltammetry behaviors (Figure 5B). As a result, these are probably due to the direct perturbation of melittin to the integrity of HBM, giving the increase of HBM permeability.

Impedance spectroscopy has been widely used to probe the electrode surface features because the interfacial electron-transfer at the electrode surface could be changed by modifying various biomaterial layers on the surface. In this work, the interfacial electron-transfer properties at the core−shell structure nanoparticles surface were altered by the adsorptions of 1-decanethiol, HBM, and different melittin concentrations. From the Figure 5C, the electron-transfer resistance at the gold surface increased upon the formation of alkanethiol and HBM layers due to the blocking

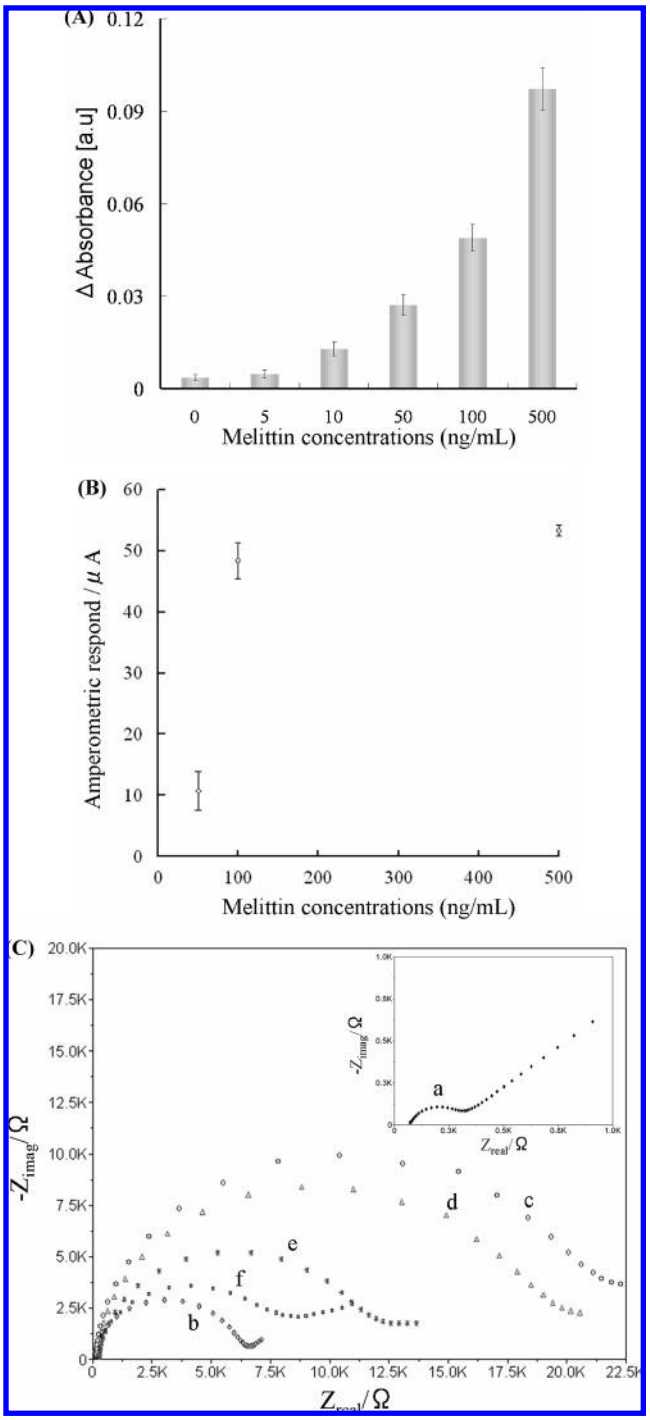

Figure 5. (A) The calibration curves for the melittin on the membrane-based sensor using localized surface plasmon resonance. (B) The relation of the amperometric response of $[Fe(CN)_6]^{3-/4-}$ with melittin concentrations. (C) Impedance plots of the core−shell structure nanoparticle substrate (a), of the thiol-modified substrate (b), of the HBM-covered substrate before (c) and after interactions with 50 ng/mL (d), 100 ng/mL (e), and 500 ng/mL (f) melittin in 1 mM $[Fe(CN)_6]^{3-/4-}$. The electrode solution contained 20 mM phosphate buffer (pH 7.4) and 100 mM KCl.

of the redox probe to the electrode surface by densely arranged successive layers. After interaction with HBM, various melittin concentration solutions caused the gradual decreases in the charge-transfer resistance, resulting from the HBM permeability increases.

CONCLUSIONS

We reported a novel membrane-based sensor to sensitively detect the presence of peptide toxin using the core−shell structure nanoparticle substrate. The binding of melittin on HBM mediated by its functionality were successively performed in the same substrate using electrochemical-localized surface plasmon resonance with the limit of detection of 10 ng/mL melittin. Up until now, there are very few studies on the interaction between melittin and a biomembrane using electrochemical methods and surface plasmon approaches. The reasons are widely considered in many aspects, especially the complex nature of interaction system and the lack of a necessary integrated chip. This work opens up the effective and trouble-free way to develop other membrane-based sensors for the detection of a huge number of functional protein toxins without using the Kretschmann configuration for surface plasmon excitation. Current works are underway to integrate this sensor into microfluids and expand it into a multiarray format to make the impact contribution to μTAS progress.

ACKNOWLEDGMENT

The authors thank Associate Professor Tsuyoshi Asahi and Assistant Professor Hiroyuki Yoshikawa from Osaka University for valuable advice during the preparations of our manuscript. Also one of these authors, H. M. Hiep, thanks Bio Device Technology Co., Ltd. (Ishikawa, Japan) for the financial support.

SUPPORTING INFORMATION AVAILABLE

Additional information as noted in text. This material is available free of charge via the Internet at http://pubs.acs.org.

Received for review January 13, 2008. Accepted February 11, 2008.

AC800087U